Optics and Laser Technology 115 (2019) 251–256

Contents lists available at ScienceDirect

Optics and Laser Technology

journal homepage: www.elsevier.com/locate/optlastec

Full length article

Solid state additive manufacture of highly-reflective Al coatings using cold spray

Richard Jenkins[a,*], Barry Aldwell[a], Shuo Yin[a], Subhash Chandra[b], Gary Morgan[c], Rocco Lupoi[a]

[a] Trinity College Dublin, The University of Dublin, Department of Mechanical and Manufacturing Engineering, Parsons Building, Dublin 2, Ireland
[b] Trinity College Dublin, The University of Dublin, Department of Civil, Structural and Environmental Engineering, Dublin 2, Ireland
[c] Enbio Ireland, DCU Alpha Innovation Campus, Old Finglas Road, Glasnevin, Dublin 11, Ireland

HIGHLIGHTS

- Cold spray can be used to fabricate highly reflective Al coatings.
- Increasing the gas heating temperature results in higher deposition efficiencies.
- Low coating densities were delivered under the highest gas heating temperatures.
- Porosity is the dominant factor that affects the reflectivity of the coatings.

ARTICLE INFO

Keywords:
Cold spray
Additive manufacturing
Reflectivity
Deposition
Aluminium

ABSTRACT

This research presents the results of an investigation into the additive manufacture of reflective Al coatings using cold spray (CS). This work is the first time that CS technology has been used to fabricate highly reflective surfaces. The coatings were characterised with respect to total reflectivity within the wavelength range of 400–1800 nm, surface roughness, particle deformation levels, and density. The experimental results indicate that raising the gas heating temperature increased the porosity and that the lowest gas heating temperature delivered the highest spectrally average reflectivity of 93.4% which was within 1% of bulk Al. This investigation demonstrates that CS can be used to coat thin layers of Al onto various materials, which can be subsequently polished to create composite reflectors. Hence, a reflector with the reflectivity of Al and the structural and thermal properties of the substrate material can be fabricated, allowing for greater design flexibility and the rapid manufacture of multi-material reflectors.

1. Introduction

Cold spray (CS) is a coating and additive manufacturing (AM) technique where metal powders with diameters in the range of 10–50 μm are accelerated to supersonic speeds using a De Laval nozzle before impacting upon a substrate [1,2]. The kinetic energy of the particle upon impact causes substantial plastic deformation of both the particle and substrate allowing bonding to occur through mechanical interlocking and adiabatic shear instability [2,3]. A schematic of the CS process with a De Laval nozzle, substrate and powder injector is shown in Fig. 1. CS allows coatings to be manufactured which show little oxide inclusion, exhibit low porosity, and are free from melting and hence adverse changes in microstructure. These attributes allow the manufacture of coatings with properties similar to those of the feedstock powder. Other distinguishing characteristics of cold spray are the ability to rapidly manufacture thick coatings or complex free-standing shapes with build rates up to an order of magnitude higher than other coating and AM technologies [4,5]. CS has been successfully applied to the deposition of a wide variety of materials for different applications including Al, Cu, Ti and their alloys, WC-Co, super-alloys, metal matrix composites and others onto various substrates including steel, Al, Cu, and others [6–17].

Al and Al-based alloys have high spectrally averaged reflectivity values (> 90%) in the visible and near-infrared wavelength range [18] which deems these materials highly suitable for the cost-effective manufacture of reflective coatings when compared to other candidates such as Ag and Au. There are a number of methods by which metallic coatings can be manufactured such as chemical vapour deposition [19], laser cladding [20], hot dipping [21], electroplating [22], sputtering [23], and the sol-gel method [24]. However, reflective coatings are

* Corresponding author.
E-mail address: jenkinsr@tcd.ie (R. Jenkins).

https://doi.org/10.1016/j.optlastec.2019.02.011
Received 2 July 2018; Received in revised form 23 October 2018; Accepted 3 February 2019
Available online 21 February 2019
0030-3992/

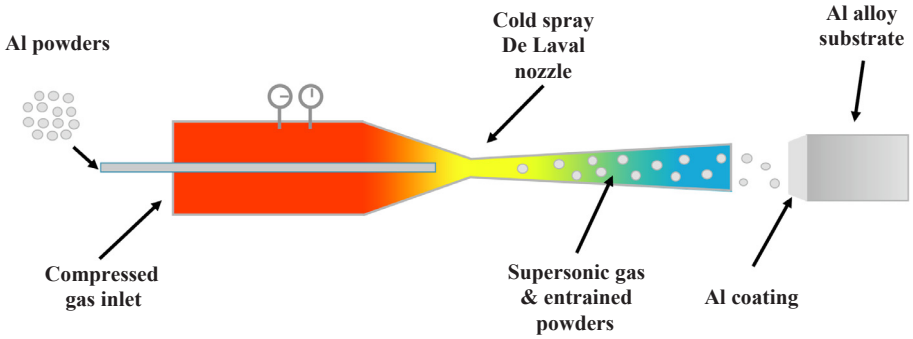

Fig. 1. Schematic of the CS additive manufacturing process.

typically manufactured with sputtering, electroplating or chemical vapour deposition which create smooth, homogenous coatings with reflectance values which approach that of the theoretical maximum of the coating material. In recent work, Zhu et al. investigated the optical properties of plasma sprayed metallic coatings of Al, Cu and Ag [25]. The results show coatings with suitable bond strength and an average reflectance value of approximately 80% over the wavelength range of 1000–2500 nm for the Al coating. Other recent work has shown that optical properties of plasma sprayed cermet coating are affected by porosity, roughness and grain boundaries [26–28].

CS, as a solid-state deposition process, has many advantages over the aforementioned manufacturing technologies. It is capable of producing coatings with high efficiency, short production time, little to no in-process oxidisation and no coating thickness limitations. Furthermore, CS is particularly suitable for producing Al coatings due to Al's ductility and low yield strength. One of the primary issues with using CS to manufacture reflective surfaces is the porous and heterogeneous nature of the coatings. Porosity will be detrimental to the optical properties of the surface by increasing roughness and provide areas for the incident radiation to become 'trapped' within the subsurface layers of the coating. However, there have been many cases of almost fully dense Al coatings being CSed with high deposition efficiencies which would make candidate reflective coatings [29,30]. Furthermore, there has been a lack of research focused on the optical properties of 'sprayed' metal coatings besides the work of Zhu [25]; thus this paper, for the first time, aims to determine if it is possible to manufacture reflective surfaces using CS and quantify the main factors which influence the optical performance of the coatings. As shown for plasma sprayed coatings, porosity, roughness and other surface defects will reduce the reflectance of the coatings and hence these factors will be the focus of in this research [25]. The gas heating temperature was the CS parameter investigated with an aim to reduce these defects by controlling the particle impact velocity.

2. Experimental setup

2.1. Coating fabrication procedure

The reflective coatings were manufactured using the in-house CS system located at Trinity College Dublin. The CS system comprises of a De Laval nozzle, gas heater, CNC system, powder feeder, computer monitoring and control system, and gas supply. Nitrogen was used as the process gas for all experiments. The gas was heated before injection into the nozzle head using a high-temperature gas heater and six gas heating temperatures ranging from 300 °C to 550 °C in 50 °C intervals were studied. The compressed gas at 30 bar is introduced into the nozzle, and the powder is fed into the nozzle throat through the powder injector. Simulated particle velocities and temperatures for the operation points were evaluated using ANSYS Fluent and are provided in Table 1. Details of the CFD computational model can be found in the author's previous work [31]. The gas and entrained powder enter the converging-diverging De Laval nozzle which accelerates the powders to supersonic speeds. High purity Al (H-30, > 99.7% Al, Valimet Inc., California) was used in this investigation at a feed rate of 60 g/min. The impurities of the H-30 powder are specified to be no more than 0.3% consisting of by weight < 0.2% Fe, < 0.2% oil and grease, and < 0.1% volatile mix. Fig. 2 shows the surface morphology and size distribution of the Al powders used which was measured using a laser diffraction particle analyser (Horiba LA 920).

Table 1
Simulated 40 μm diameter particle velocities and temperatures on impact with the substrate.

Gas	Gas temperature (°C)	Pressure (bar)	Particle velocity (m/s)	Particle temp (°C)
N_2	300	30	641	182
N_2	350	30	661	222
N_2	400	30	680	263
N_2	450	30	699	303
N_2	500	30	718	344
N_2	550	30	733	383

A nozzle cooling jacket was employed during this investigation (similar to the device used by Wang et al. [32]) to prevent clogging of the nozzle at high temperatures. The coatings were sprayed onto 30 mm diameter × 25 mm height billets of Al 6082 T6 alloy substrate which had an average surface roughness of approximately 500 nm after machining. The choice of the substrate was primarily a function of the ease of manufacture of the billets and material availability; however, other substrates could equally be used for this application as the adhesion of Al to various metals, polymers and ceramic with high bond strength has been widely reported [15–17,29,30,33,34]. All samples were sprayed at a traverse speed of 100 mm/s and a step size of 5 mm using a bidirectional strategy. The number of passes on each sample was controlled to obtain a coating thickness of approximately 1.5 mm. Post cold spray, the coating thickness was reduced through grinding and polishing to approximately 0.5 mm thickness to remove the rough, undulating surface and to ensure that first layer interactions with the substrate would not affect the coating characteristics.

2.2. Coating characterisation

Before reflectivity and surface roughness was measured, the samples were finished using a Jean Wirtz Phoenix 4000 polishing machine. Samples were ground/polished using P180 grit, P1200 grit, 6 μm diamond suspension, 1 μm diamond suspension, and 0.06 μm colloidal silica suspension for a total time of 1–2 min (until the correct coating thickness was obtained), 3 min, 3 min and 10 min respectively at 150 rpm and 2 bar sample pressure. The polishing process was developed based on the recommended procedure and materials from MetPrep (UK). Unpolished samples were not evaluated due to the unsuitable nature of the rough surface for use as a reflector in the as-

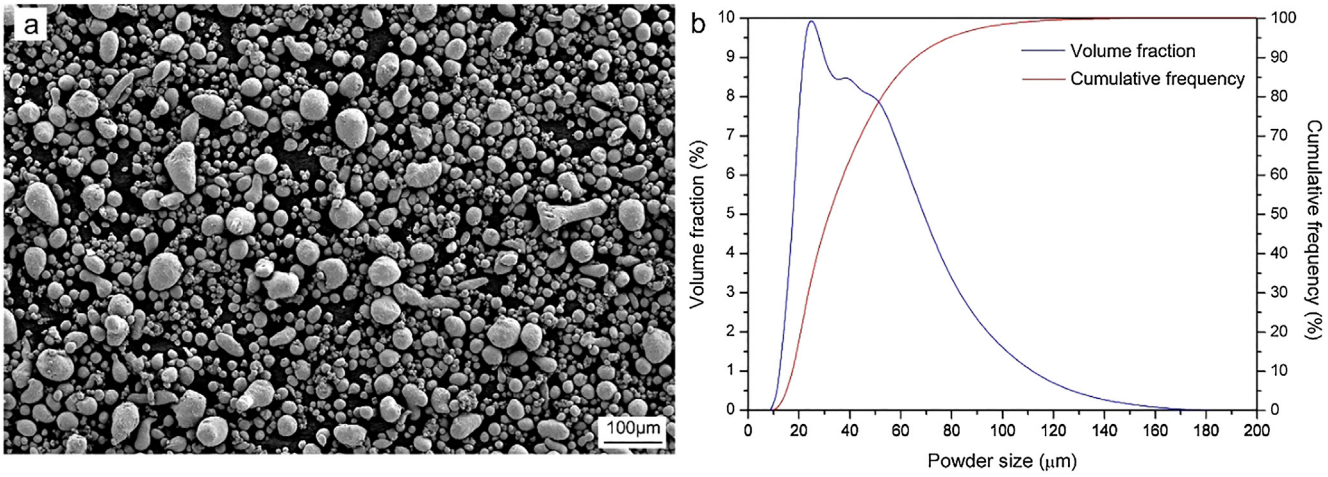

Fig. 2. Feedstock powders (a) surface morphology, and (b) particle size distribution.

fabricated state. Reflectivity measurements were carried out using Perkin Elmer Lambda 900 between the visible and near-IR wavelength range of 400 to 1800 nm in steps of 0.5 nm with the UV/Visible and near-IR detector change occurring at 860 nm. The sample's spectrally averaged reflectance was calculated as the mean reflectance value across the wavelength range tested. Finally, the measurement error of the spectrometer was determined to ± 0.65% by obtaining five spectrally averaged measurements of a single Al sample.

The average surface roughness (S_a) of the polished coatings were measured using a white light interferometer (WLI, Filmetrics, Profilm 3D) using a magnification of 10×. Five images randomly located on the surface were averaged to find the S_a using the standard ISO 25178. Porosity was also inferred from relative density measurements carried out based on the Archimedes principle using the following formula:

$$\rho_{relative} = \frac{\rho_{coating}}{\rho_{bulk}} = \frac{\rho_{water} \bullet m_{coating(air)}}{\rho_{bulk} \bullet (m_{coating(air)} - m_{coating(water)})}$$

where $\rho_{coating}$ is the density of the CS sample; ρ_{bulk} is the measured density of a bulk Al sample which was determined to be 2.71 g/cm^3 using the same method; $m_{coating(air)}$ is the weight of CS sample in air; $m_{coating(water)}$ is the weight of CS sample in water; ρ_{water} is the density of water. The CS samples were removed from the billets using a lathe after removal of the top surface to produce a 'coin' shape from which the density can be accurately measured. A single deposition efficiency measurement for each process parameters was determined using the ratio of the deposit weight to the total weight of powder delivered through the powder feeder for a 40-second spray time. Coating cross sections were characterised in the SEM by first mounting and polishing using a similar polishing procedure used for the reflective samples. Etching was carried out by exposing coating cross sections to Keller's reagent for 2–3 min. The flattening ratio is a measure of particle deformation and is defined as the ratio of the diameter of a splat to the diameter of a sphere of the same volume [2,35]. The flattening ratio was determined from SEM images of etched cross-sections of three representative gas heating temperatures using 10 randomly selected particles that had clearly identifiable boundaries.

3. Results and discussion

3.1. Reflectivity and coating microstructure

The total reflectivity vs wavelength data of selected polished samples and the bulk Al comparison is shown in Fig. 3, while a photograph of a polished cold sprayed Al surface at 300 °C is also included. Notably, the reflectance of all of the coatings drastically drops at 800 nm which corresponds to the reported absorption band of Al [36]. Overall, there is

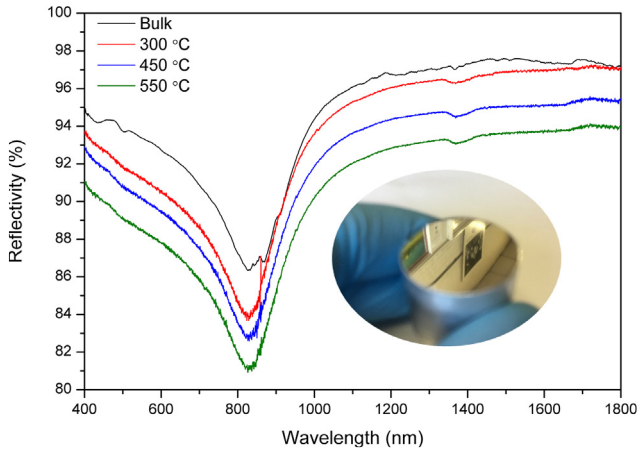

Fig. 3. Total reflectivity data for various gas heating temperatures and bulk Al with polished sample preparation. An image of 300 °C gas heating CS sample is also shown.

a clear trend between the CS gas heating temperature and the coating reflectance for the samples shown: the surface reflectance incrementally decreases with an increase in gas heating temperature across the entire wavelength range. The 550 °C sprayed sample had the lowest average reflectance while the 300 °C sprayed sample had the highest average reflectance with the 450 °C sample bisecting the two curves. In addition, the bulk Al sample has the highest reflectance of all the tests as expected due to the lack of surface porosity and defects. The reflectance of the bulk Al sample compares well with published literature for Al at room temperature with a local minimum at 826 nm of approximately 86% (vs 86.3%) and a local maximum of 96% (vs 97.2%) at 1800 nm [36]. The 300 °C sprayed sample has a reflectance quite close to that of the bulk sample throughout the near infrared wavelength range. However, the difference between the samples is more significant in the UV range. This may be due to the presence of small-scale defects on the surface of the coatings which absorb incoming radiation more prominently in the UV range than the near IR range. Shorter wavelength will be absorbed or scattered more readily than longer wavelengths as given by Mie theory.

The spectrally averaged reflectance of each sample versus gas heating temperature is provided in Fig. 4. The maximum average reflectance was 93.4% for the 300 °C, and the minimum average reflectance was 90.4% for the 550 °C sample indicating that a lower gas heating temperature is optimal for producing highly reflective coatings with this setup. The remaining samples followed a somewhat linear

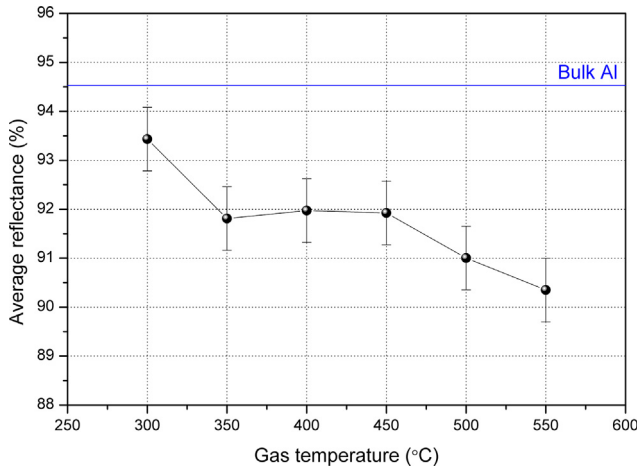

Fig. 4. Average reflectance values versus the gas temperature.

decrease as the gas heating temperature was increased with the exception of the 350 °C sample. Note: the difference between each of the samples was visually quite clear with the highest reflectance sample appearing very close to a mirror with only minor surface defects while with the 500 °C surface defects were apparent throughout the surface. The reflectance values provided in Fig. 4 show that a highly reflective surface can be manufactured with CS which approaches the reflectance of that of bulk Al with the bulk sample being 1.2% more reflective than the coating sprayed at 300 °C. The difference between the samples is not within the experimental uncertainty of the spectrometer (± 0.65%) but, overall, is quite insignificant in terms of absolute reflectance. In the authors' opinion, with further work and improved selection of powders, cold sprayed reflective surfaces with the reflectivity of bulk Al are achievable. This will be discussed further in section 3.2. When compared to the data presented by Zhu et al. [25], the highest reflectance is a significantly improved with 93% reflectance at 400–1800 nm versus 80% at 1000–2500 nm, although it must be considered that no post process polishing was carried out by Zhu et al. in their research.

In order to understand the reflectivity trend, polished, etched and etched binary counterpart cross-sectional SEM images of a selection of samples are presented in Fig. 5. It is clear that there is an increase in porosity of the coatings as the gas heating temperature is increased as there are pores and defects visible throughout the coating at the highest gas heating temperature tested (550 °C, Fig. 5c). This supports the reflectivity data in Fig. 4 as an increase in surface porosity will obviously lead to decreased optical performance. The etched cross sections and corresponding binary images (Fig. 5d–i) show substantial deformation of the particles at the lowest gas heating temperatures tested and comparatively less deformation as the gas heating temperature is increased. In order for inter-particle voids to be filled and a dense coating manufactured, it is critical that high strain rate deformation occurs upon particle impact and impact from subsequent particles [37]. The flatting ratio is a measure of deformation and was determined to be 1.98, 1.89 and 1.74 for the gas heating temperatures of 300 °C, 400 °C and 550 °C respectively which highlights the disparity in deformation which occurs across the range of gas heating temperatures tested. It is clear that particle deformation and highly dense coatings lead to improved reflectivity as pores and defects will promote the indecent radiation becoming 'trapped' within the subsurface layers of the coating instead of reflecting upon the upper reflective surface.

3.2. Effect of coating porosity and surface roughness on the coating reflectance

From Fig. 5, it is apparent that the porosity of the coating increases with gas heating temperature; however, the variation in porosity across the coating surface can lead to large uncertainties when quantifying using 2D cross-sectional images. Therefore, the porosity was measured using the Archimedes water balance method which accounts of the entire volume of the coating and thus is a more representative approach with lower uncertainty. Fig. 6 shows the effect of gas heating temperature on the coating porosity and deposition efficiency. The porosity data supports the reflectivity data in Fig. 4 and the cross-sectional images in Fig. 5 as an increasing porosity level will result in a greater probability of absorption of incident radiation within surface defects. The lowest bulk porosity of 0.72% corresponded with the highest average reflectance (93.4%) and the highest bulk porosity measurement also corresponded with the lowest reflectance value measured (90.4%), highlighting porosity's influence on reflectance. Typically, when CSing high-ductility materials (such as Cu), increasing the gas heating temperature and pressure will reduce the coating porosity due to the increased particle impact velocities [38]. However, in this work, the experimental results indicate that the coating porosity of CS Al increases with increasing the gas heating temperature. The trend shown in this investigation is due to the enhanced particle tamping effect which occurs under low deposition efficiency which can result in the densification of porous coatings [39–41]. A detailed description of the mechanism that causes this trend is outside of the scope of this investigation, and there can be found in the author's previous publication [42].

As expected, an increase in gas heating temperature increases deposition efficiency which is typical of cold spray: increasing the gas temperature will enhance the sonic velocity of the gas and in turn increases the particle impact velocity. This allows more particles to exceed the critical velocity and deposit to form a coating. Additionally, the heated gas transfers thermal energy to the in-flight particles which reduces the critical velocity through thermal softening. Increased deposition efficiency is favourable as the processing cost is reduced and the build rate increased: the deposition efficiency rose from 5% to 23% for gas heating temperatures of 300 °C and 550 °C respectively as shown in Fig. 6. However, the porosity of the coatings also increased within this temperature range. The coating porosity should be minimised to increase optical performance, and hence the lowest gas heating temperature test is the optimal operating point. However, this set point is inefficient in terms of gas and powder usage as the majority of powder exiting the nozzle fails to bond with the substrate or coating. The literature provides many examples of deposition efficiencies of above 60% at 700 m/s for pure Al which is in contrast to the deposition efficiency of 15% obtained in this experiment at similar velocities [29,30]. Smaller powders with a more favourable size range were utilised in the aforementioned references, and therefore it may be the case that an improved powder selection is required for future work on this topic.

Porosity, among other factors, will influence the surface roughness of the coatings, as the craters associated with bulk porosity will result in surfaces that are below that of the mean S_a value. This will tend to increase the value of S_a, but the deviations are due to porosity rather than random variation upon the top surface. With a rough undulating surface (large S_a value), incident radiation is more likely to be absorbed due to multiple reflections on the surface; thus a smoother surface is preferential to increase the total reflectivity. In addition, for specular reflectivity, a smooth surface is also required to ensure incident radiation reflects at the consistent angle to maintain image directionality. Due to the heterogeneous nature of CS coatings with porosity, there is variation in roughness across the surface which poses great difficulty in measuring S_a with a high degree of certainty even at low magnifications; therefore five randomly located images were taken on each of the surfaces to determine average surface roughness and reduce uncertainty. Fig. 7 shows the gas heating temperature versus surface roughness and reflectivity. There is no clear relationship for the gas heating temperature versus surface roughness data besides the maximum S_a value corresponding the minimum reflectance; the S_a actually

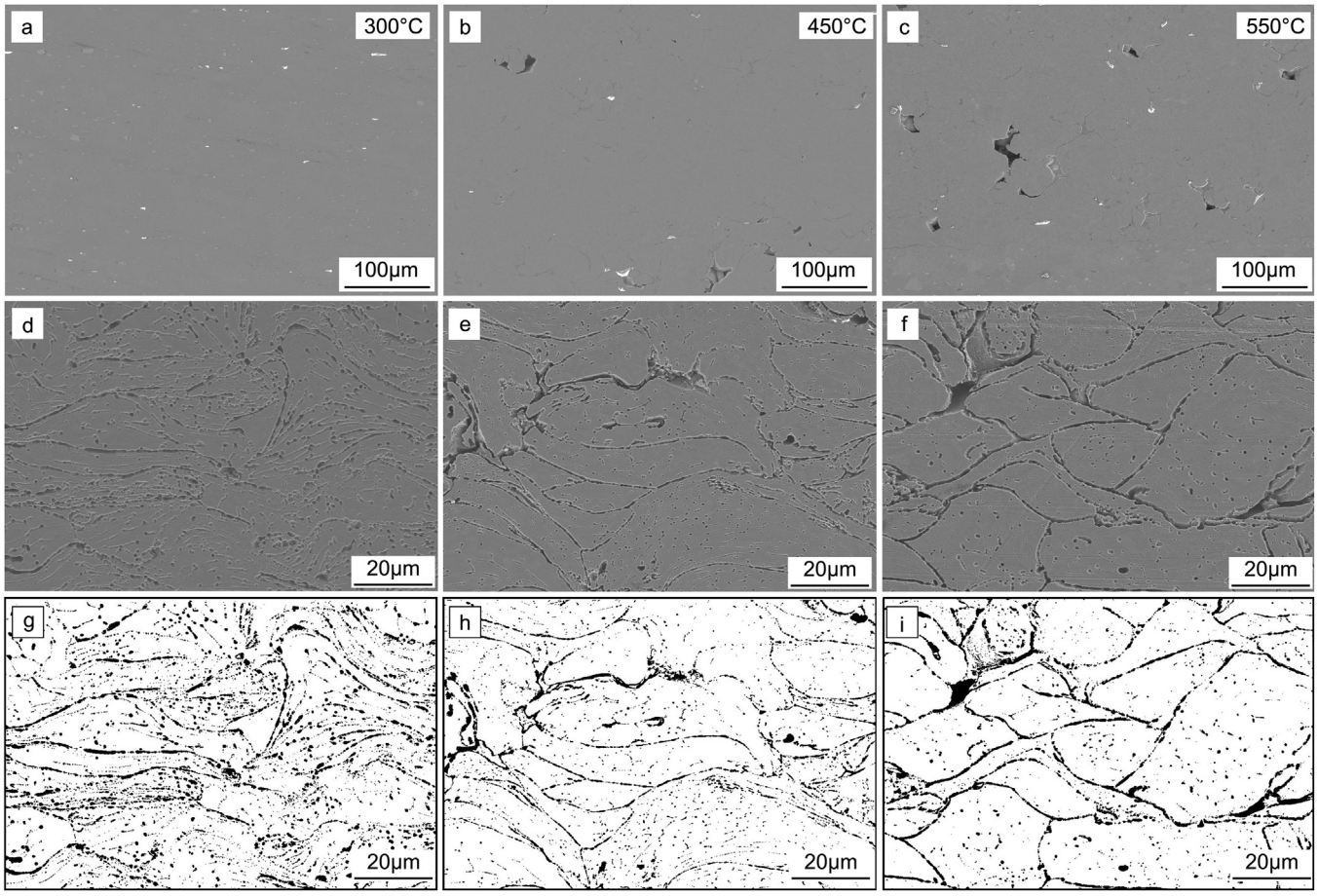

Fig. 5. Cross-sectional SEM images of coatings produced at 300 °C, 400 °C and 550 °C. (a–c) polished cross-sections, (d–f) etched cross sections and (g–i) etched binary counterparts.

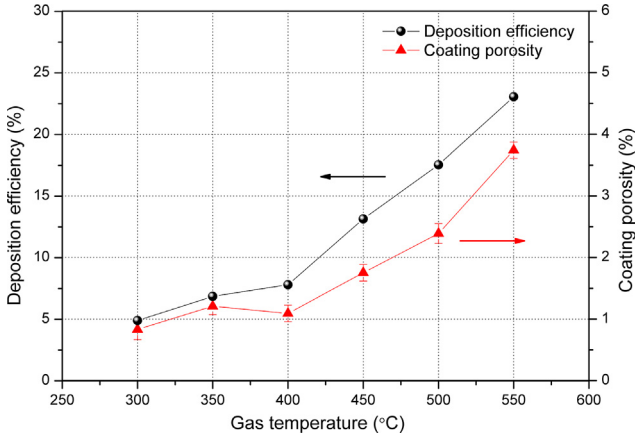

Fig. 6. Coating porosity and deposition efficiency versus the gas temperature.

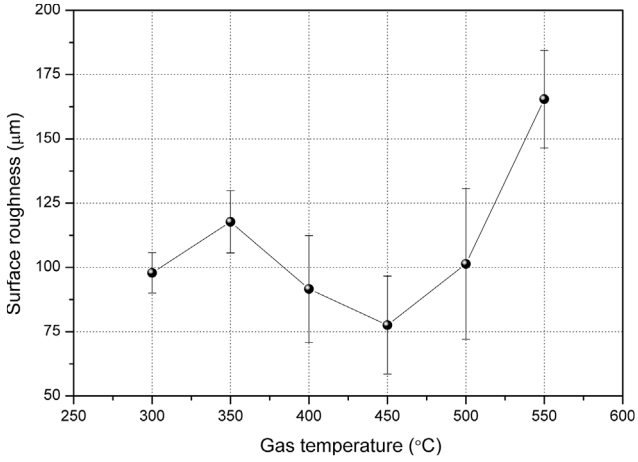

Fig. 7. Surface roughness and average reflectance versus the gas temperature.

decreased as the gas heating temperature was increased from 350 °C to 450 °C. The minimum S_a value obtainable will be determined by the polishing procedure, the mechanical properties of the material and, as discussed, the surface porosity. However, the primary factor which will limit the lowest surface roughness obtainable for CS coatings will be the porosity as pores cannot be removed or reduced through polishing. In addition, due to the significant disparity between the top surface roughness and the depth of surface pores and the steep angles of the pore walls, the WLI could not accurately capture the entire pore, and this missing data was filled during post-processing which results in the inaccurate measurement of the surface roughness. Therefore, the surface roughness cannot be accurately quantified by the WLI when measuring a highly porous surface with steep crater walls such as is found at the highest gas heating temperatures. However, it can be concluded that surface porosity is the dominant factor which determines the reflectivity of a CS coating and S_a should be used as a surface quality metric when comparing highly dense coatings with little surface porosity.

4. Conclusions

Several Al coatings were cold sprayed using commercially pure feedstock at various gas heating temperature. The primary aim of the investigation is the discovery of the effect of CS parameters on the optical properties of the coatings, and hence the coatings were quantified with respect to reflectance, porosity and surface roughness. The reflectance of the coatings sprayed at the lowest gas heating temperatures approached the reflectivity of bulk Al (93.4% vs 94.5%), and higher reflectance values could be achieved with follow-on work and improvements to the selection of feedstock powder. The CS coatings with higher porosity were shown to decrease the reflectance of the surfaces, and the porosity of the coatings increased from 0.72% to 4.44% for the lowest and highest gas heating temperatures respectively. Porosity was found to be the dominant factor which influences the surface roughness and hence reflectivity of the coating. Finally, this research has shown that highly reflective coatings that approach the optical performance of bulk materials can be additively manufactured using cold spray with build rates significantly higher than competing techniques.

Acknowledgments

This work was supported by the European Space Agency (4000112844/14/NL/FE) and Irish Research Council (GOIPD-2017-912).

Appendix A. Supplementary material

Supplementary data to this article can be found online at https://doi.org/10.1016/j.optlastec.2019.02.011.

References

[1] V.K. Champagne, The Cold Spray Materials Deposition Process: Fundamentals and Applications, Elsevier, 2007.
[2] H. Assadi, F. Gärtner, T. Stoltenhoff, H. Kreye, Bonding mechanism in cold gas spraying, Acta Mater. 51 (2003) 4379–4394.
[3] T. Schmidt, H. Assadi, F. Gärtner, H. Richter, T. Stoltenhoff, H. Kreye, T. Klassen, From particle acceleration to impact and bonding in cold spraying, J. Therm. Spray Technol. 18 (2009) 794–808.
[4] J. Pattison, S. Celotto, R. Morgan, M. Bray, W. O'Neill, Cold gas dynamic manufacturing: a non-thermal approach to freeform fabrication, Int. J. Mach. Tools Manuf. 47 (2007) 627–634, https://doi.org/10.1016/J.IJMACHTOOLS.2006.05.001.
[5] S. Yin, P. Cavaliere, B. Aldwell, R. Jenkins, H. Liao, W. Li, R. Lupoi, Cold spray additive manufacturing and repair: fundamentals and applications, Addit. Manuf. 21 (2018) 628–650, https://doi.org/10.1016/j.addma.2018.04.017.
[6] S. Yin, Y. Xie, J. Cizek, E.J. Ekoi, T. Hussain, D.P. Dowling, R. Lupoi, Advanced diamond-reinforced metal matrix composites via cold spray: properties and deposition mechanism, Compos. Part B Eng. 113 (2017) 44–54, https://doi.org/10.1016/j.compositesb.2017.01.009.
[7] D. Goldbaum, J.M. Shockley, R.R. Chromik, A. Rezaeian, S. Yue, J.-G. Legoux, E. Irissou, The effect of deposition conditions on adhesion strength of Ti and Ti6Al4V cold spray splats, J. Therm. Spray Technol. 21 (2012) 288–303.
[8] C. Stenson, K.A. McDonnell, S. Yin, B. Aldwell, M. Meyer, D.P. Dowling, R. Lupoi, Cold spray deposition to prevent fouling of polymer surfaces, Surf. Eng. (2016) 1–11, https://doi.org/10.1080/02670844.2016.1229833.
[9] B. Aldwell, S. Yin, K.A. McDonnell, D. Trimble, T. Hussain, R. Lupoi, A novel method for metal–diamond composite coating deposition with cold spray and formation mechanism, Scr. Mater. 115 (2016) 10–13, https://doi.org/10.1016/j.scriptamat.2015.12.028.
[10] T. Marrocco, T. Hussain, D.G. McCartney, P.H. Shipway, Corrosion performance of laser posttreated cold sprayed titanium coatings, J. Therm. Spray Technol. 20 (2011) 909–917.
[11] A.S.M. Ang, C.C. Berndt, P. Cheang, Deposition effects of WC particle size on cold sprayed WC–Co coatings, Surf. Coatings Technol. 205 (2011) 3260–3267.
[12] P.-H. Gao, C.-J. Li, G.-J. Yang, Y.-G. Li, C.-X. Li, Influence of substrate hardness transition on built-up of nanostructured WC–12Co by cold spraying, Appl. Surf. Sci. 256 (2010) 2263–2268.
[13] P. Poza, C.J. Múnez, M.A. Garrido-Maneiro, S. Vezzù, S. Rech, A. Trentin, Mechanical properties of Inconel 625 cold-sprayed coatings after laser remelting. Depth sensing indentation analysis, Surf. Coatings Technol. 243 (2014) 51–57.
[14] D. Seo, M. Sayar, K. Ogawa, SiO 2 and MoSi 2 formation on Inconel 625 surface via SiC coating deposited by cold spray, Surf. Coatings Technol. 206 (2012) 2851–2858.
[15] J. Affi, H. Okazaki, M. Yamada, M. Fukumoto, Fabrication of aluminum coating onto CFRP substrate by cold spray, Mater. Trans. 52 (2011) 1759–1763.
[16] X. Wu, J. Zhang, X. Zhou, H. Cui, J. Liu, Advanced cold spray technology: deposition characteristics and potential applications, Sci. China Technol. Sci. 55 (2012) 357–368.
[17] E. Irissou, J.-G. Legoux, A.N. Ryabinin, B. Jodoin, C. Moreau, Review on cold spray process and technology: Part I—Intellectual property, J. Therm. Spray Technol. 17 (2008) 495–516, https://doi.org/10.1007/s11666-008-9203-3.
[18] M. Bass, E.W. van Stryland, D.R. Williams, W.L. Wolfe, OSA Handbook of Optics, vol. 2, 1995.
[19] H.O. Pierson, Knovel (Firm), Handbook of chemical vapor deposition principles, technology, and applications, Mater. Sci. Process Technol. Ser. Electron. Mater. Process Technol. xxiv (1999) 482, https://doi.org/10.1016/B978-081551432-9.50006-1.
[20] E. Toyserkani, A. Khajepour, S.F. Corbin, Laser Cladding, CRC Press, 2004.
[21] F.W. Bach, A. Laarmann, T. Wenz, Modern Surf. Technol. (2006), https://doi.org/10.1002/3527608818.
[22] M. Schlesinger, M. Paunovic, Modern Electroplating: Fifth Ed. (2011), https://doi.org/10.1002/9780470602638.
[23] K. Wasa, S. Hayakawa, Kiyotaka Wasa, Shigeru Hayakawa, K. Wasa, S. Hayakawa, Kiyotaka Wasa, Shigeru Hayakawa, Handbook of sputter deposition, Technol.: Princ. Technol. Appl. (1992), https://doi.org/10.1016/B978-1-4377-3483-6.00006-1.
[24] G. Vijayaprasath, R. Murugan, T. Mahalingam, Y. Hayakawa, G. Ravi, Preparation of highly oriented Al:ZnO and Cu/Al:ZnO thin films by sol-gel method and their characterization, J. Alloys Compd. 649 (2015) 275–284, https://doi.org/10.1016/j.jallcom.2015.07.089.
[25] J. Zhu, Z. Ma, L. Gao, Y. Liu, F. Wang, Influence of microstructure on the optical property of plasma-sprayed Al, Cu, and Ag coatings, Mater. Des. 111 (2016) 192–197.
[26] V. Debout, A. Vardelle, P. Abelard, P. Fauchais, E. Meillot, E. Bruneton, F. Enguehard, S. Schelz, Investigation of in-flight particle characteristics and microstructural effects on optical properties of YSZ plasma-sprayed coatings, High Temp. Mater. Process: Int. Q. High-Technol. Plasma Process. (2007) 11.
[27] J. Marthe, E. Meillot, G. Jeandel, F. Enguehard, J. Ilavsky, Enhancement of scattering and reflectance properties of plasma-sprayed alumina coatings by controlling the porosity, Surf. Coatings Technol. 220 (2013) 80–84, https://doi.org/10.1016/j.surfcoat.2012.05.048.
[28] L. del Campo, D. De Sousa Meneses, K. Wittmann-Ténèze, A. Bacciochini, A. Denoirjean, P. Echegut, Effect of porosity on the infrared radiative properties of plasma-sprayed yttria-stabilized zirconia ceramic thermal barrier coatings, J. Phys. Chem. C 118 (2014) 13590–13597.
[29] Q. Wang, N. Birbilis, M.-X. Zhang, Process optimisation of cold spray Al coating on AZ91 alloy, Surf. Eng. 30 (2014) 323–328, https://doi.org/10.1179/1743294413Y.0000000224.
[30] J. Won, G. Bae, K. Kang, C. Lee, S.J. Kim, K.A. Lee, S. Lee, Bonding, reactivity, and mechanical properties of the kinetic-sprayed deposition of Al for a thermally activated reactive Cu liner, J. Therm. Spray Technol. 23 (2014) 818–826, https://doi.org/10.1007/s11666-014-0088-z.
[31] M.C. Meyer, S. Yin, K.A. McDonnell, O. Stier, R. Lupoi, Feed rate effect on particulate acceleration in Cold Spray under low stagnation pressure conditions, Surf. Coatings Technol. 304 (2016) 237–245.
[32] X. Wang, B. Zhang, J. Lv, S. Yin, Investigation on the clogging behavior and additional wall cooling for the axial-injection cold spray nozzle, J. Therm. Spray Technol. 24 (2015) 696–701, https://doi.org/10.1007/s11666-015-0227-1.
[33] R. Jenkins, S. Yin, B. Aldwell, R. Lupoi, T. Lupton, R. Jenkins, A.J.J. Robinson, G.E.E. O'Donnell, Direct manufacturing of diamond composite coatings onto silicon wafers and heat transfer performance, CIRP Ann. (2018), https://doi.org/10.1016/j.cirp.2018.04.092.
[34] J. Villafuerte, Corrosion protection of magnesium by cold spray, Magnes. Alloy. Surf. Treat. InTech, 2011.
[35] V.K. Champagne, D.J. Helfritch, M.D. Trexler, B.M. Gabriel, The effect of cold spray impact velocity on deposit hardness, Model. Simul. Mater. Sci. Eng. 18 (2010) 65011.
[36] J. Bartl, M. Baranek, Emissivity of aluminium and its importance for radiometric measurement, Meas. Sci. Rev. 4 (2004) 31–36.
[37] M.R. Rokni, S.R. Nutt, C.A. Widener, V.K. Champagne, R.H. Hrabe, Review of relationship between particle deformation, coating microstructure, and properties in high-pressure cold spray, J. Therm. Spray Technol. 26 (2017) 1308–1355.
[38] P.S. Phani, D.S. Rao, S.V. Joshi, G. Sundararajan, Effect of process parameters and heat treatments on properties of cold sprayed copper coatings, J. Therm. Spray Technol. 16 (2007) 425–434.
[39] Y. Hao, J. qiang Wang, X. yu Cui, J. Wu, T. fan Li, T. ying Xiong, Microstructure characteristics and mechanical properties of Al-12Si coatings on AZ31 magnesium alloy produced by cold spray technique, J. Therm. Spray Technol. 25 (2016) 1020–1028, https://doi.org/10.1007/s11666-016-0409-5.
[40] Y.-K. Wei, X.-T. Luo, C.-X. Li, C.-J. Li, Optimization of in-situ shot-peening-assisted cold spraying parameters for full corrosion protection of Mg alloy by fully dense al-based alloy coating, J. Therm. Spray Technol. 26 (2017) 173–183, https://doi.org/10.1007/s11666-016-0492-7.
[41] X.T. Luo, Y.K. Wei, Y. Wang, C.J. Li, Microstructure and mechanical property of Ti and Ti6Al4V prepared by an in-situ shot peening assisted cold spraying, Mater. Des. 85 (2015) 527–533, https://doi.org/10.1016/j.matdes.2015.07.015.
[42] R. Jenkins, S. Yin, B. Aldwell, M. Meyer, R. Lupoi, New insights into the in-process densification mechanism of cold spray Al coatings: low deposition efficiency induced densification, J. Mater. Sci. Technol. (2018).